Effect of reactive magnesia on erosion control of a lead contaminated lean clay: insights from runoff, infiltration and disintegration characteristics

Zhengtao Shen[1]*[#], Yue Xu[2#], Yuanyuan Geng[3], Fei Jin[4], Benyi Cao[5], Huan Liu[6], Chao-Sheng Tang[7], Bin Shi[8]

Information of the authors

1. School of Earth Sciences and Engineering, Nanjing University, Nanjing 210023, China. E-mail: ztshen@smail.nju.edu.cn

2. School of Earth Sciences and Engineering, Nanjing University, Nanjing 210023, China. E-mail: 522022290024@smail.nju.edu.cn

3. School of Earth Sciences and Engineering, Nanjing University, Nanjing 210023, China. E-mail: 502022290067@smail.nju.edu.cn

4. School of Engineering, Cardiff University, Cardiff CF24 3AA, UK, E-mail: jinf2@cardiff.ac.uk

5, School of Engineering, University of Surrey, Guildford GU2 7XH, UK, E-mail: b.cao@surrey.ac.uk

6. School of Earth Sciences and Engineering, Nanjing University, Nanjing 210023, China. E-mail: liuhuan@nju.edu.cn

7. School of Earth Sciences and Engineering, Nanjing University, Nanjing 210023, China. E-mail: tangchaosheng@nju.edu.cn

8. School of Earth Sciences and Engineering, Nanjing University, Nanjing 210023, China. E-mail: shibin@nju.edu.cn

*Corresponding author:

Zhengtao Shen, E-mail: ztshen@nju.edu.cn

#These authors contribute equally to this work

Abstract: The erosion-induced environmental risks of contaminated soil and the corresponding remediation strategies remain inadequately understood. This study investigates the effect of reactive magnesia (MgO), a low-carbon and highly effective remediation material, on erosion control of lead (Pb)-contaminated silty clay, focusing on runoff, infiltration and disintegration characteristics. This study found that the co-migration of Pb with soil particles via runoff is the primary pathway for its transport. MgO treatment decreases the chemically dissolved Pb concentration in runoff by 71%, and the mass of Pb-contaminated soil loss to runoff erosion by 92.4%. Furthermore, MgO treatment lowers the clay content in eroded soil particles from 17% in the parent soil to 7%, reduces their Pb concentration from 4960 mg/kg to 3600 mg/kg, and increases their proportion of stable Pb from 79% to 96%, thereby substantially mitigating the environmental risk posed by eroded soil particles. Further hydro-mechanical analysis reveals that MgO significantly delays the onset of disintegration in Pb-contaminated soil and reduces the final disintegration rate from 100% to 35%. This study presents a new perspective on balancing chemical stabilisation with physical solidification for the remediation of heavy metal-contaminated soils.

Keywords: Pb contaminated soil; erosion control; Pb migration; chemical stabilisation; soil solidification; reactive magnesia

Notation List

MgO	Reactive magnesia
Pb	Lead
V_{tn}	The disintegration rate of the sample at a given immersion time
m_n	The mass of disintegrated soil particles at a given immersion time
M	The total mass of the sample
δ_{tn}	The disintegration ratio of the sample

1 Introduction

Lead (Pb) is a toxic heavy metal that can cause irreversible damage to the brain, nervous system, and cardiovascular system of human beings, particularly in children and pregnant women (O'Connor et al., 2020). According to the "Global Burden of Disease Study 2019", global Pb exposure contributes to approximately 9 million deaths each year (Fuller et al., 2022). Pb pollution primarily originates from the improper disposal of lead-acid batteries and electronic waste (Akram et al., 2019), mining and smelting of Pb-containing minerals (Forsyth et al., 2019), and Pb-containing waste generated during the production of paints and pigments (Ranjbar et al., 2023). Since Pb is non-biodegradable in nature, it persists in the environment and accumulates into soil through the food chain, posing a significant threat to ecosystems (Angon et al., 2024). Soil acts as a major sink for Pb (Raj and Das, 2023), playing a crucial role in mitigating its mobility and bioavailability in the environment.

Natural process, such as rainfall cycles, can facilitate Pb leaching from soil, leading to its migration (Kushwaha et al., 2018, Zhang et al., 2024). Rainwater generally exhibits a pH of 5.6, and acid rain has an even lower pH (Prakash et al., 2023), reducing Pb solubility in soil. Consequently, it is widely believed that long-term exposure to rainwater causes Pb dissolution in soil, thereby posing environmental risks (Qi et al., 2022). However, the physical effects of rainwater are often overlooked. In fact, Pb in contaminated soil can also migrate to surrounding areas via co-migration with rainfall-eroded soil particles (Wang et al., 2024a). Studies have shown that the concentration of heavy metals in sediments transported by surface runoff is 2.31-3.98 times higher than that in the parent contaminated soil (Quinton and Catt, 2007, Shen et al.,

2021).

Chemical stabilisation is the most widely used method for the remediation of Pb-contaminated soils (Wang et al., 2021a, Du et al., 2014a). This technique involves incorporating materials such as biochar, phosphates, and reactive magnesia (MgO) into the soil (Wang et al., 2021b, Xu et al., 2021). These additives promote adsorption, complexation, and precipitation of Pb, thereby enhancing its stability within the soil matrix and inhibiting migration. Among these materials, MgO has emerged as a promising Pb remediation agent due to its high efficiency, durability and lower carbon emissions compared to Portland cement, a conventional soil remediation material (Li et al., 2019, Cao et al., 2023, Yi et al., 2014). Several studies have demonstrated that MgO effectively reduces the chemical leaching of metals under laboratory and field conditions using batch leaching tests (Wang et al., 2018, Yi et al., 2014, Wang et al., 2016). However, it remains unclear whether MgO can effectively mitigate Pb leaching caused by erosion and the co-migration of Pb with soil particles. Evaluating the efficacy of MgO under the dynamic environmental conditions is crucial to understanding its dual role in chemical stabilisation and erosion control of heavy-metal-contaminated soils.

In this study, MgO was used to remediate Xiashu soil (a lean clay) severely contaminated with Pb. This soil is representative of surface soils from one of China's key heavy metal contamination regions - the middle and lower reaches of the Yangtze Plain. Using simulated rainwater erosion experiments, this study explored the patterns and mechanisms of MgO's effects on Pb-contaminated Xiashu soil from three perspectives: runoff, infiltration, and disintegration characteristics. By integrating chemical stabilisation and erosion control, this

study provides theoretical support and practical guidance for effective remediation of Pb-contaminated soils.

2 Materials and methods

2.1 Materials

The soil used in this study is Xiashu soil, which is widely distributed in the middle and lower reaches of the Yangtze River plain, China. Xiashu soil is classified as a low-plasticity clay, with its primary clay minerals comprising interstratified illite-smectite (61.8%), illite (32.1%), and kaolinite (6.1%). Table 1 presents the basic properties of Xiashu soil.

Xiashu soil was collected from the topsoil (0-25 cm) in Pukou District, Nanjing, China. The collected soil was air-dried at room temperature for 14 days. Subsequently, it was crushed and sieved through a 2 mm mesh to remove plant roots, gravel, and other non-soil components. A $Pb(NO_3)_2$ solution with a designated Pb concentration was thoroughly mixed with a certain amount of the sieved soil to achieve a Pb concentration of 5000 mg/kg, simulating severely Pb-contaminated soil based on the national standard for soil environmental quality (GB 36600-2018). The prepared Pb-contaminated soil was incubated at a water content of 40% for 7 days to ensure the uniform distribution of Pb within the soil. It was then oven-dried at 40 °C for 48 hours, re-crushed, and sieved through a 2 mm mesh for sample preparation.

The MgO used in this experiment is a light-burned MgO, which is produced based on HG/T2573-2012. It has a pH of 10.3 and reactivity of 30 s, determined by the method described in Jin and Al-Tabbaa (2014).

106 **2.2 Sample preparation and experimental design**

107 MgO was added to the Pb-contaminated soil at dosages of 0%, 5% and 10%, respectively
108 (Table 2). Briefly, MgO was thoroughly mixed with the sieved Pb-contaminated soil, and
109 deionised water was added to achieve a water content of 19%. The soils were then sealed and
110 incubated for 2 days. Subsequently, the soils were statically compacted in a mold at a constant
111 rate of 0.4 mm/min, forming compacted soil samples with dimensions of 16 × 16 × 5 cm and a
112 dry density of 1.5 g/cm^3. Each sample contained 768 g of soil and 3840 mg of Pb, irrespective
113 of the MgO addition. Deionised water was sprayed onto the prepared samples to maintain a
114 water content of 30% to avoid either too dry or too wet, and the samples were then sealed and
115 incubated for 7 days.

116 The soil erosion experiment was conducted following the method described by Shen et al.
117 (2021). As illustrated in Fig. 1, the prepared samples were placed on a platform with the slope
118 adjusted to 15° to facilitate the collection of surface runoff. The samples were housed in an
119 acrylic box measuring 16 × 16 × 8 cm, featuring 49 drainage holes with a diameter of 2 mm at
120 the bottom. Two layers of filter paper were lined to regulate the rainfall intensity. An 8 mm-
121 diameter outlet was installed at a height of 3.5 cm (corresponding to the sample's upper surface)
122 and at the bottom of the box to collect runoff and infiltration, including soil particles in both
123 flows.

124 The rainfall intensity and duration were set to 12 mm/h and 1 h to simulate short-duration
125 heavy rainfall extremes based on the national standard for rainfall levels (GB/T 28592-2012).
126 After each rainfall simulation, the samples were air-dried for 71 hours at room temperature. A

total of 16 rainfall cycles, each lasting 72 h, were conducted to simulate the extreme rainfall events likely to occur over a four-year period in Nanjing based on the information at the China Meteorological Data Service Center (https://data.cma.cn/). After each cycle, photographs of the sample surface were taken to examine the erosion conditions, and runoff and infiltration were collected and analysed. The control soil sample (M0) fully penetrated and interconnected by rainwater after the fifth rainfall cycle, leading to the discontinuation of testing for the M0 sample beyond this cycle.

2.3 Physical and chemical analysis

The collected runoff and infiltration solutions were left to settle at room temperature for 24 hours, after which the clear supernatant was carefully collected to record the volume. The supernatant was then filtered through a 0.45 μm filter and the Pb concentration was measured using an inductively coupled plasma optical emission spectrometer (ICP-OES) with a detection limit of 0.03 mg/L. The sedimented soil particles were retrieved through filtration, and weighed after oven drying at 40 °C until a constant weight was reached. The particle size distribution of the soil particles was analysed by a laser particle size analyser (Mastor2000). The total Pb concentration of the soil particles was determined by microwave digestion, dilution and filtration, followed by ICP-OES analysis. All analyses were conducted in triplicates, with the mean values and standard deviations reported.

2.4 Disintegration test

To further investigate the hydro-mechanical stability of the Pb-contaminated soils with and without MgO treatment, a disintegration test was conducted following the method

described by Tang et al. (2023). The sample specifications were consistent with those in Table 2 and were formed into cubes measuing 2.5 × 2.5 × 2.5 cm. The collection device consists of a plastic water tank and a 2000 mL beaker. The disintegration cage is slightly smaller than the beaker and featured a mesh screen with a 2 mm pore size at the bottom to facilitate the collection of soil particles after disintegration. The test was conducted in triplicate.

Before the experiment, the water tank and 10 beakers were filled with water, and the samples were placed in the disintegration cage. The disintegration cage was submerged sequentially in the corresponding beakers for specific immersion times: 5 s, 10 s, 30 s, 1 min (60 s), 5 min (300 s), 10 min (600 s), 1 h (3600 s), 1.5 h (5400 s), 3 h (10800 s), and 12 h (43200 s). After the experiment, the beakers were removed from the water tank, and the dry mass of the soil particles collected from each beaker was measured. The mass represented the disintegrated soil at each time interval. The disintegration rate and ratio at different immersion times were calculated using Eq (1) and Eq (2):

$$V_{tn} = \frac{m_n}{M} \times 100\% \quad (1)$$

$$\delta_{tn} = \sum_1^n \frac{m_n}{M} \times 100\% \quad (2)$$

where V_{tn} represents the disintegration rate of the sample at a given immersion time, m_n denotes the mass of disintegrated soil particles at a given immersion time, M is the total mass of the

168 sample, and δ_{tn} signifies the disintegration ratio of the sample.

169 **3 Results and discussion**

170 **3.1 Runoff**

171 ***Runoff volume***

172 The runoff volumes in M5 and M10 were significantly higher than in M0, and higher MgO
173 dosage resulted in higher runoff volumes (Fig. 2a&b). For instance, the runoff volumes of M5
174 and M10 were 24.2% and 31.5% higher than that in M0 after the first cycle. This increase in
175 runoff may be attributed to the hydration of MgO, which enhances bonding among soil particles
176 and strengthens the soil structure. Consequently, more rainfall accumulated on the surface as
177 runoff due to reduced soil permeability. As the number of cycles increased, the individual runoff
178 volumes of the samples gradually increased and eventually stabilised. This may be attributed
179 to: (1) the soils being unsaturated at the start of the experiment, leading to initial absorption of
180 rainwater and reduced runoff; (2) the simulated rainfall continuously compacting the soils,
181 progressively decreasing their permeability and reaching a stable state.

182 ***Pb leaching in runoff***

183 MgO treatment significantly reduced Pb leaching in the run-off at the first cycle (Fig. 3a).
184 Compared to M0 (0.677 mg/L), the Pb concentration in run-off for M5 and M10 decreased to
185 0.230 mg/L (by 66%) and 0.199 mg/L (by 71%), respectively. After the first cycle, the effect of
186 MgO treatment on Pb leaching in the run-off became insignificant. From the forth cycle onward,
187 Pb in the run-off was negligible for all samples. The decrease in Pb concentration in the runoff

with increasing cycles is due to the leaching of weakly bound Pb during the earlier cycles, and the remaining Pb in the soil is more stable and less prone to leaching in subsequent cycles (Tessier et al., 1979). The individual leached Pb amounts in the runoff followed the same trend as their concentrations (Fig. 3b). After 16 cycles, the cumulative leached Pb amounts in the runoff were 1.53 mg for M0 (calculated only up to the forth cycle), 1.36 mg for M5, and 1.13 mg for M10.

Erosion of Pb contaminated soil in runoff

MgO treatment significantly reduce the loss of Pb-contaminated soil through run-off (Fig. 4). For instance, the eroded soil mass for M5 and M10 reduced by 81.6% and 92.4% respectively, compared to M0 at the first cycle. Under the effect of rainfall, the erosion of M0 gradually increased until the sample failed after the fifth cycle. In total, 189 g of soil was eroded, accounting for 25% of its initial mass. In contrast, the MgO-treated samples experienced minimal soil erosion throughout the cycles, with M10 showing almost no erosion beyond the first cycle. The solidifying effect of MgO on the soil is also evident in the surface morphology of the samples (Fig. 5). The surface of M0 was significantly damaged by rainwater erosion, while the surface damage of M5 was notably reduced. In contrast, the surface morphology of M10 exhibited almost no visible change.

Compared to the control, the eroded soil in the runoff had significantly higher sand fraction and lower clay fraction after MgO treatment (Fig. 6). Because clay and silt particles exhibit higher reactivity, they are more readiliy cemented and stabilised by MgO (Spadini et al., 2018). As the eroded soil contains more sand, and sand has a much lower capacity to carry heavy

metals compared to clay and silt (Wu et al., 2024), the Pb concentration in the eroded soils treated with MgO are significantly lower (3920 mg/kg for M5 and 3500 mg/kg for M10) than that of the control (4960 mg/kg)(Fig. 7a). Due to the immobilisation by MgO, the Pb in eroded soil for M10 is rendered more stable than that in the untreated soil (Fig. 7b).

3.2 Infiltration

Infiltration volume

The infiltration volumes of all samples were significantly lower than their run-off volumes (Fig. 2). Higher MgO dosage resulted in significantly lower infiltration volumes, because the expansion of hydrated MgO reduces soil porosity and permeability, preventing rainwater infiltration (Ben-Moshe et al., 2013, Bayat et al., 2019). Interestingly, M5 showed a higher infiltration volume than M0, which may be due to the insufficient expansion of MgO upon hydration to fully fill soil voids for M5, resulting in higher permeability. Additionally, the hydration product (i.e., magnesium hydroxide) encapsulated the soil particles, limiting their ability to absorb water, reducing their water-holding capacity (Wang et al., 2018, Wang et al., 2021a). Consequently, rainwater rapidly infiltrates through the remaining pores, leading to higher infiltration. In contrast, with higher MgO content, the pores are predominantly filled by the hydrated MgO, impeding water infiltration and leading to lower infiltration for M10.

Pb leaching in infiltration

The concentration of Pb in infiltration was generally higher than that in runoff. This may be attributed to the more extensive interaction between water and the Pb-contaminated soil

during infiltration, as well as the longer residence time compared to runoff processes. This extended contact allows Pb within the soil to desorb into the water more effectively (Rassaei, 2023). MgO did not significantly reduce the concentrations of Pb in M5 and M10 compared to M0 during the first four cycles (Fig. 3d). In fact, after the forth cycle, M10 exhibited a higher Pb concentration in the infiltration solution (1.660 mg/L) than M0 (0.666 mg/L). As the infiltration volume was significantly smaller than the runoff volume, the total amount of Pb leached in infiltration during a single cycle was less than 0.1 mg/L (Fig. 3e). The relatively higher cumulative amount of Pb leached through infiltration for M5 compared with M0 and M10 was due to its higher infiltration volume (Fig. 3f). However, the cumulative amount of Pb leached through infiltration for all samples remained significantly lower than that leached through runoff (Fig. 3f).

Loss of Pb contaminated soil in infiltration

The loss of Pb-contaminated soil due to infiltration was significantly lower than that caused by runoff for all samples (Table 3). At the first cycle, MgO treatments reduced the migration of Pb in contaminated soil via infiltration by 82% (M5) and 92% (M10), respectively, compared to M0. After the forth cycle, no further loss of Pb from the contaminated soil was detected from infiltration. Given the relatively low overall risk of Pb migration through infiltration, no further analyses (e.g., particle size or Pb concentration) were conducted.

3.3 Disintegration characteristics

The Pb-contaminated soil without MgO treatment rapidly disintegrated upon submersion (Fig. 8a), reaching a 96% disintegration ratio within 1005 s (Fig. 8b). In contrast, M5 and M10

exhibited significantly delayed disintegration, with the process commencing only after 1005s of immersion. Their disintegration rates were also slower, requiring significantly more time (>20805 s) to reach their maximum disintegration. The final disintegration ratios for M5 and M10 were 66% and 35%, respectively. MgO significantly improves the water stability of the Pb-contaminated soil, and higher dosages further enhance this improvement.

3.4 Discussion

Rainfall induced Pb migration

Numerous studies indicate that rainwater can chemically dissolve heavy metals, thereby facilitating their migration and posing environmental risks (Xu et al., 2024, Ouyang et al., 2017, Rao et al., 2016). The findings of this study align with these observations. Specifically, runoff induced by rainwater dissolved approximately 1.53 mg of Pb (equivalent to 1.99 mg/kg in 768 g of total dry soil), whereas infiltration dissolved about 0.11 mg of Pb (0.14 mg/kg in 768 g of total dry soil) (Fig. 3c&f). From a chemical dissolution perspective, horizontal migration via runoff represents the primary environmental risk for the Pb-contaminated silty clay. It is noteworthy that although the proportion of Pb dissolved through runoff was small in this experiment, circumneutral (pH 6.5) deionised water was used over only 16 simulated rainfall cycles. Under field conditions with acid rain over a longer duration (Du et al., 2014b), the risk of Pb migration through runoff could be considerably higher.

This study revealed that horizontal co-migration of Pb with soil particles induced by runoff erosion may pose a greater risk than dissolved-phase Pb migration. Before the sample was fully penetrated, just five rainfall cycles resulted in the runoff-driven erosion of 180 g of Pb

contaminated soil, accounting for 23% of the total dry mass of the sample (Fig. 4b). In large metal-mining areas - particularly those with slopes and cohesive soils (e.g., Hunan, Guangxi, and Yunnan in China) (Shi et al., 2023) - even if Pb migration via dissolution is not substantial, the co-migration of Pb and soil particles due to erosion warrants serious attention. For these specific regions, remediation efforts may need to shift from purely chemical stabilisation to methods that enhance the mechanical properties of soil. The risk of Pb co-migration with soil particles through infiltration was notably lower than that via runoff erosion (Table 4). Considering the experimental limitations, such as the sample thickness (2 cm) and the presence of 49 small holes (diameter of 2 mm) in the base (resulting in an overestimation of seepage-induced soil loss), the real-world infiltration risk of Pb co-migration with soil particles is likely even lower under field conditions.

Effectiveness of MgO in prevention of Pb migration

This study presents compelling evidence that MgO effectively inhibits the migration of Pb: (1) MgO significantly decreases the leaching of Pb into runoff; (2) MgO substantially reduces the erosion of Pb-contaminated soil, thereby lowering the risk of Pb co-migration with eroded soils; (3) the eroded soil after MgO treatment contains significantly less Pb, and the remaining Pb is considerably more stable compared to the parent soil; and (4) MgO markedly enhances the hydro-mechanical stability of Pb-contaminated soil, delaying the disintegration process and reducing the cumulative disintegration ratio. These findings provide deeper insights into the mechanisms by which MgO prevents Pb migration, compared to existing literature that primarily uses batch leaching methods (e.g., TCLP) to assess the stability of MgO-stabilised

metals (Wang et al., 2018, Wang et al., 2021a, Shen et al., 2019b). In other words, beyond chemical stabilisation, enhancing the water stability and erosion resistance of soil can also significantly contribute to inhibiting Pb migration. It should be noted that the prevention of Pb migration by MgO is more pronounced at a dosage of 10%. Although MgO effectively inhibits Pb migration overall, adding 5% MgO increases the total amount of Pb leached through infiltration. Therefore, practical applications should carefully consider the optimal dosage of MgO to maximise its inhibitory effects while minimizing unintended consequences.

Implications for soil remediation

Soil erosion is a prevalent phenomenon in natural environments. In mining areas, metal extraction activities often alter the topography, leading to the formation of sloping tailings deposits that are frequently associated with heavy metal contamination (Grangeia et al., 2011, Emel et al., 2014). Previous studies have primarily focused on the chemical migration of heavy metals (Sun et al., 2022, Wang et al., 2024b). However, erosion can facilitate a more extensive co-migration of heavy metals with soil particles. Therefore, in such regions, the risk of heavy metal migration due to erosion cannot be overlooked.

Since the 1980s, cement-based solidification/stabilisation techniques have been the primary method for the remediation of heavy metal-contaminated soils (Shen et al., 2019a). However, starting around 2010, cement has been increasingly recognised as a high-carbon emission material (Miller et al., 2018), prompting a shift towards reducing its usage (Shen et al., 2019a). Consequently, in the context of heavy metal remediation - especially in emerging soil remediation markets such as China - chemical stabilisation methods utilizing biochar, clay

minerals, iron-based and phosphate-based materials have gained prominence (Ma et al., 2022). Although chemical stabilisation can effectively immobilise heavy metals through efficient chemical reactions (e.g., complexation and precipitation), it has minimal impact on the mechanical properties of soil. Based on the findings of this study, the extensive application of chemical stabilisation may pose a risk of heavy metals co-migrating through erosion processes. Therefore, in regions with significant erosion risks, it is essential to consider soil solidification in addition to heavy metal immobilisation to mitigate the risk of heavy metal migration caused by erosion.

4 Conclusion

This study investigates the effect of MgO on the erosion control of the Pb-contaminated silty clay based on runoff, infiltration and disintegration characteristics. It is found that soil loss induced by erosion, along with the associated co-migration of Pb with soil particles, poses the primary environmental risk, significantly exceeding the risk of Pb leaching caused by chemical dissolution in rainwater. The risk of Pb migration through infiltration is negligible. MgO mitigates the risk of Pb migration through multiple mechanisms. It reduces the Pb concentration in runoff (from chemical dissolution) by up to 71% and decreases the mass of Pb-contaminated soil loss to runoff erosion by 92.4%, thereby substantially mitigating the co-migration of Pb with soil particles, identified here as the predominant environmental hazard. Furthermore, MgO lowers the clay content in eroded soil particles from 17% in the parent soil to 7%, reduces the Pb concentration from 4960 mg/kg to 3600 mg/kg, and increases the proportion of stable Pb from 79% to 96%, significantly decreasing the environmental risk posed by eroded soil particles.

Hydro-mechanical analysis further indicates that MgO significantly delays the onset of disintegration in Pb-contaminated soil and reduces the final disintegration rate from 100% (untreated) to 35%. These findings were achieved using a 10% MgO application, whereas the effect of adding 5% MgO was considerably less pronounced. By elucidating the mechanisms underlying MgO remediation of Pb-contaminated silty clay, this study provides valuable insights into the treatment of regionally contaminated soils (e.g., metal tailings and soils surrounding mining areas) and offers a new perspective for balancing chemical stabilisation with physical solidification in the remediation of heavy metal-contaminated soils.

Acknowledgments

This work was supported by the National Key Research and Development Program of China (2023YFC3707900), the Fundamental Research Funds for the Central Universities (2024300399), National Natural Science Foundation of China (42277123, 42477187), Natural Science Foundation of Jiangsu Province (BK20220787).

References

Akram, R., Natasha, Fahad, S., Hashmi, M. Z., Wahid, A., Adnan, M., Mubeen, M., Khan, N., Rehmani, M. I. A., Awais, M., Abbas, M., Shahzad, K., Ahmad, S., Hammad, H. M. & Nasim, W. (2019) Trends of electronic waste pollution and its impact on the global environment and ecosystem. *Environmental Science and Pollution Research* **26(17)**:16923-16938.

Angon, P. B., Islam, M. S., Shreejana, K. C., Das, A., Anjum, N., Poudel, A. & Suchi, S. A. (2024) Sources, effects and present perspectives of heavy metals contamination: Soil, plants and human food chain. *Heliyon* **10(7)**.

Bayat, H., Kolahchi, Z., Valaey, S., Rastgou, M. & Mahdavi, S. (2019) Iron and magnesium nano-oxide effects on some physical and mechanical properties of a loamy Hypocalcic Cambisol. *Geoderma* **335**:57-68.

Ben-Moshe, T., Frenk, S., Dror, I., Minz, D. & Berkowitz, B. (2013) Effects of metal oxide nanoparticles on soil properties. *Chemosphere* **90(2)**:640-6.

Cao, B., Xu, J., Wang, F. & Al-Tabbaa, A. (2023) Self-healing soil mix cutoff wall materials incorporating reactive MgO pellets. *Géotechnique* **74(12)**:1317-1328.

Du, Y. J., Jiang, N. J., Liu, S. Y., Jin, F., Singh, D. N. & Puppala, A. J. (2014a) Engineering properties and microstructural characteristics of cement-stabilized zinc-contaminated kaolin. *Canadian Geotechnical Journal* **51(3)**:289-302.

Du, Y. J., Wei, M. L., Reddy, K. R., Liu, Z. P. & Jin, F. (2014b) Effect of acid rain pH on leaching behavior of cement stabilized lead-contaminated soil. *Journal of Hazardous Materials* **271**:131-140.

Emel, J., Plisinski, J. & Rogan, J. (2014) Monitoring geomorphic and hydrologic change at mine sites using satellite imagery: The Geita Gold Mine in Tanzania. *Applied Geography* **54**:243-249.

Forsyth, J. E., Nurunnahar, S., Islam, S. S., Baker, M., Yeasmin, D., Islam, M. S., Rahman, M., Fendorf, S., Ardoin, N. M., Winch, P. J. & Luby, S. P. (2019) Turmeric means "yellow" in Bengali: Lead chromate pigments added to turmeric threaten public health across Bangladesh. *Environ Res* **179(Pt A)**:108722.

Fuller, R., Landrigan, P. J., Balakrishnan, K., Bathan, G., Bose-O'reilly, S., Brauer, M., Caravanos, J., Chiles, T., Cohen, A., Corra, L., Cropper, M., Ferraro, G., Hanna, J., Hanrahan, D., Hu, H., Hunter, D., Janata, G., Kupka, R., Lanphear, B., Lichtveld, M., Martin, K., Mustapha, A., Sanchez-Triana, E., Sandilya, K., Schaefli, L., Shaw, J., Seddon, J., Suk, W., Tellez-Rojo, M. M. & Yan, C. (2022) Pollution and health: a progress update. *Lancet Planet Health* **6(6)**:e535-e547.

Grangeia, C., Avila, P., Matias, M. & Da Silva, E. F. (2011) Mine tailings integrated investigations: The case of Rio tailings (Panasqueira Mine, Central Portugal). *Engineering Geology* **123(4)**:359-372.

Jin, F. & Al-Tabbaa, A. (2014) Characterisation of different commercial reactive magnesia. *Advances in cement research* **26(2)**:101-113.

Kushwaha, A., Hans, N., Kumar, S. & Rani, R. (2018) A critical review on speciation, mobilization and toxicity of lead in soil-microbe-plant system and bioremediation strategies. *Ecotoxicol Environ Saf* **147**:1035-1045.

Li, W., Ni, P. & Yi, Y. (2019) Comparison of reactive magnesia, quick lime, and ordinary Portland cement for stabilization/solidification of heavy metal-contaminated soils. *Sci Total Environ* **671**:741-753.

Ma, Y., Wang, L. N., Cao, Y. Z., Liang, T., Wang, P. P., Luo, H. L., Yu, J. J., Zhang, D. D., Xing, B. S. & Yang, B. (2022) Stabilization and remediation of heavy metal-contaminated soils in China: insights from a decade-long national survey. *Environmental Science and Pollution Research* **29(26)**:39077-39087.

Miller, S. A., John, V. M., Pacca, S. A. & Horvath, A. (2018) Carbon dioxide reduction potential in the global cement industry by 2050. *Cement and Concrete Research* **114**:115-124.

O'connor, D., Hou, D., Ok, Y. S. & Lanphear, B. P. (2020) The effects of iniquitous lead exposure on health. *Nature Sustainability* **3(2)**:77-79.

Ouyang, W., Huang, W. J., Hao, X., Tysklind, M., Haglund, P. & Hao, F. H. (2017) Watershed soil Cd loss after long-term agricultural practice and biochar amendment under four rainfall levels. *Water Research* **122**:692-700.

Prakash, J., Agrawal, S. B. & Agrawal, M. (2023) Global Trends of Acidity in Rainfall and Its Impact on Plants and Soil. *Journal of Soil Science and Plant Nutrition* **23(1)**:398-419.

Qi, S. Q., Li, X. X., Luo, J., Han, R. F., Chen, Q. Q., Shen, D. S. & Shentu, J. (2022) Soil heterogeneity influence on the distribution of heavy metals in soil during acid rain infiltration: Experimental and numerical modeling. *Journal of Environmental Management* **322**.

Quinton, J. N. & Catt, J. A. (2007) Enrichment of heavy metals in sediment resulting from soil erosion on agricultural fields. *Environmental Science & Technology* **41(10)**:3495-3500.

Raj, K. & Das, A. P. (2023) Lead pollution: Impact on environment and human health and approach for a sustainable solution. *Environmental Chemistry and Ecotoxicology* **5**:79-85.

Ranjbar, Z., Pourhadadi, D., Montazeri, S. & Modaberi, M. R. (2023) Lead compounds in paint and coatings: A review of regulations and latest updates. *Progress in Organic Coatings* **174**.

Rao, Z. X., Huang, D. Y., Zhu, H. H., Zhu, Q. H., Wang, J. Y., Luo, Z. C., Xu, C., Shen, X. & He, Y. B. (2016) Effect of rice straw mulching on migration and transportation of Cd, Cu, Zn, and Ni in surface runoff under simulated rainfall. *Journal of Soils and Sediments* **16(8)**:2021-2029.

Rassaei, F. (2023) Adsorption Kinetics and Isotherm Modeling of Lead in Calcareous Soils: Insights into Thermodynamics, Desorption, and Soil Properties. *Communications in Soil Science and Plant Analysis* **54(15)**:2059-2076.

Shen, Z., Jin, F., O'connor, D. & Hou, D. (2019a) Solidification/stabilization for soil remediation: an old technology with new vitality.) ACS Publications.

Shen, Z., Pan, S., Hou, D., O'connor, D., Jin, F., Mo, L., Xu, D., Zhang, Z. & Alessi, D. S. (2019b) Temporal effect of MgO reactivity on the stabilization of lead contaminated soil. *Environment International* **131**:104990.

Shen, Z. T., Zhang, Z. R., Zhang, M. D., Rinklebe, J., Ma, Y. & Hou, D. Y. (2021) Effect of production temperature and particle size of rice husk biochar on mercury immobilization and erosion prevention of a mercury contaminated soil. *Journal of Hazardous Materials* **420**.

Shi, J. D., Zhao, D., Ren, F. T. & Huang, L. (2023) Spatiotemporal variation of soil heavy metals in China: The pollution status and risk assessment. *Science of the Total Environment* **871**.

Spadini, L., Navel, A., Martins, J. M. F., Vince, E. & Lamy, I. (2018) Soil aggregates: a scale to

investigate the densities of metal and proton reactive sites of organic matter and clay phases in soil. *European Journal of Soil Science* **69(5)**:953-961.

Sun, R. G., Gao, Y. & Yang, Y. (2022) Leaching of heavy metals from lead-zinc mine tailings and the subsequent migration and transformation characteristics in paddy soil. *Chemosphere* **291**.

Tang, C., Pan, X., Cheng, Y. & Ji, X. (2023) Improving hydro-mechanical behavior of loess by a bio-strategy. *Biogeotechnics* **1(2)**.

Tessier, A., Campbell, P. C. & Bisson, M. (1979) Sequential extraction procedure for the speciation of particulate trace metals. *Analytical Chemistry* **51(7)**:844-851.

Wang, F., Jin, F., Shen, Z. & Al-Tabbaa, A. (2016) Three-year performance of in-situ mass stabilised contaminated site soils using MgO-bearing binders. *Journal of Hazardous Materials* **318**:302-307.

Wang, F., Li, W., Wang, H., Hu, Y. & Cheng, H. (2024a) The leaching behavior of heavy metal from contaminated mining soil: The effect of rainfall conditions and the impact on surrounding agricultural lands. *Sci Total Environ* **914**:169877.

Wang, F., Li, W., Wang, H., Hu, Y. N. & Cheng, H. F. (2024b) The leaching behavior of heavy metal from contaminated mining soil: The effect of rainfall conditions and the impact on surrounding agricultural lands. *Science of the Total Environment* **914**.

Wang, F., Shen, Z. & Al-Tabbaa, A. (2018) PC-based and MgO-based binders stabilised/solidified heavy metal-contaminated model soil: strength and heavy metal speciation in early stage. *Géotechnique* **68(11)**:1025-1030.

Wang, F., Xu, J., Zhang, Y. H., Shen, Z. T. & Al-Tabbaa, A. (2021a) MgO-GGBS Binder-Stabilized/Solidified PAE-Contaminated Soil: Strength and Leachability in Early Stage. *Journal of Geotechnical and Geoenvironmental Engineering* **147(8)**.

Wang, L. W., Rinklebe, J., Tack, F. M. G. & Hou, D. Y. (2021b) A review of green remediation strategies for heavy metal contaminated soil. *Soil Use and Management* **37(4)**:936-963.

Wu, Y. L., Yang, J. J., Chang, R. Q., Li, S. C. & Kou, H. L. (2024) Strength, leaching characteristics and microstructure of CGF plus P all-solid-waste binder solidification/stabilization Cu(II) contaminated soil. *Construction and Building Materials* **411**.

Xu, D. M., Fu, R. B., Wang, J. X., Shi, Y. X. & Guo, X. P. (2021) Chemical stabilization remediation for heavy metals in contaminated soils on the latest decade: Available stabilizing materials and associated evaluation methods-A critical review. *Journal of Cleaner Production* **321**.

Xu, Z. X., Yin, M., Yang, X., Yang, Y., Xu, X. H., Li, H. G., Hong, M., Qiu, G. H., Feng, X. H., Tan, W. F. & Yin, H. (2024) Simulation of vertical migration behaviors of heavy metals in polluted soils from arid regions in northern China under extreme weather. *Science of the Total Environment* **919**.

Yi, Y., Li, C., Liu, S. & Al-Tabbaa, A. (2014) Resistance of MgO-GGBS and CS-GGBS stabilised marine soft clays to sodium sulfate attack. *Géotechnique* **64(8)**:673-679.

Zhang, L., Zhu, Y., Gu, H., Lam, S. S., Chen, X., Sonne, C. & Peng, W. (2024) A review of phytoremediation of environmental lead (pb) contamination. *Chemosphere* **362**:142691.

Table captions

Table 1 Basic properties of Xiashu soil used in this work

Table 2 Mix proportions and sample notations used in this work

Table 3 Mass of soil loss in infiltration at different rainfall cycles

Figure captions

Fig. 1. Schematic diagram of the soil erosion experiment (Shen et al., 2021).

Fig. 2. Runoff (a-individual, b-cumulative) and infiltration (c-individual, d-cumulative) volumes of the soils with and without MgO treatment.

Fig. 3. Pb leaching in the runoff (a-individual concentration, b-individual amount, c-cumulative amount) and infiltration (c-individual concentration, d-individual amount, f-cumulative amount).

Fig. 4. Erosion induced loss of Pb-contaminated soil (a-individual rainfall, b-cumulative).

Fig. 5. Effect of MgO on surface morphology of Pb-contaminated soil during rainfall cycles.

Fig. 6. Particle size distribution of the eroded Pb-contaminated soil in runoff.

Fig. 7. Pb concentration (a) and fraction (b) of eroded soil in runoff.

Fig. 8. Disintegration rate (a) and ration (b) of Pb contaminated soil.

489 Table 1 Basic properties of Xiashu soil used in this work

Parameter	Value
Specific gravity	2.73
Grain size distribution	
Sand content (%)	2
Silt content (%)	76
Clay content (%)	22
Atterberg limits	
Liquid limits	36.5
Plastic limits	19.5
Plasticity index	17.0
Standard compaction test	
Optimum moisture content (%)	16.5
Maximum dry density (g/cm^3)	1.7
Optimum water content (%)	16.5
USCS classification (ASTM 2017)	Lean clay (CL)

490

491 Table 2. Mix proportions and sample notations used in this work

Sample ID	Density (g/ cm^3)	Water content (w/w)	MgO dosage (%)	Pb concentration (mg/kg)
M0	1.5	30	0	5000
M5	1.5	30	5	5000
M10	1.5	30	10	5000

492

493 Table 3. Mass of soil loss in infiltration at different rainfall cycles

Rainfall cycle	M0(g)	M5(g)	M10(g)
1	18.48	3.40	1.40
4	64.46	2.43	0
8	0	0	0
12	0	0	0
16	0	0	0

494

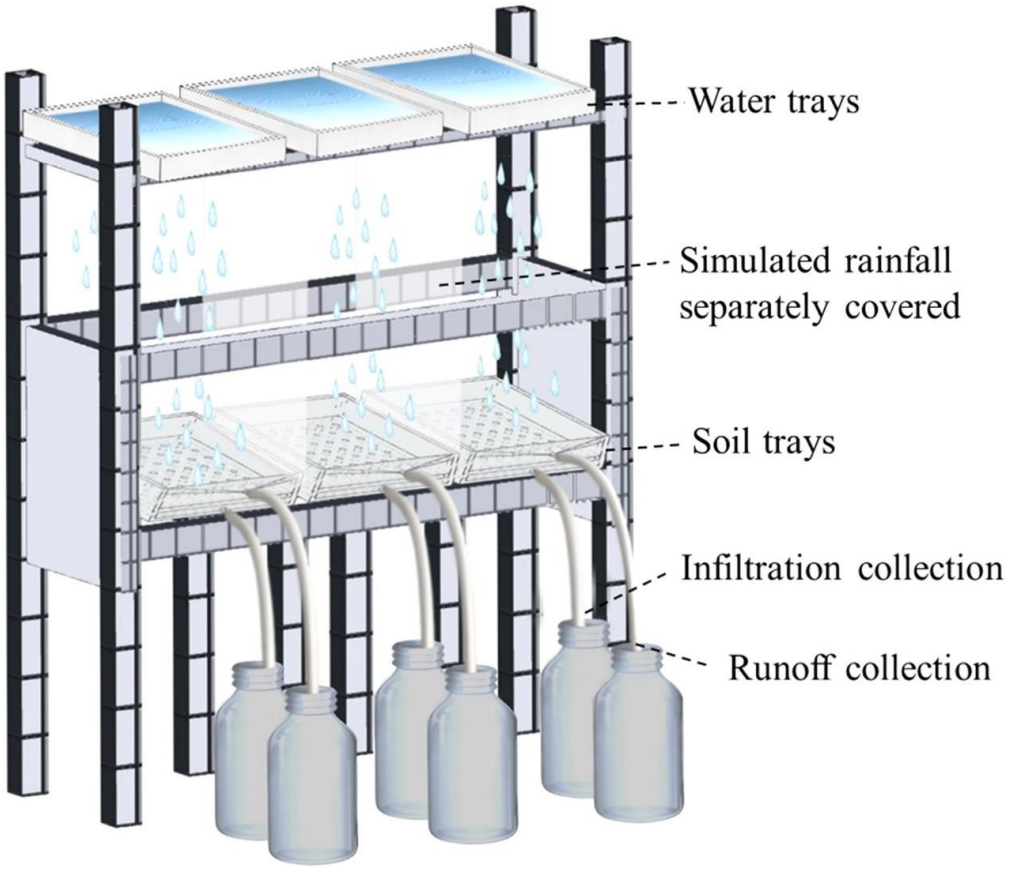

Fig. 1. Schematic diagram of the soil erosion experiment (Shen et al., 2021).

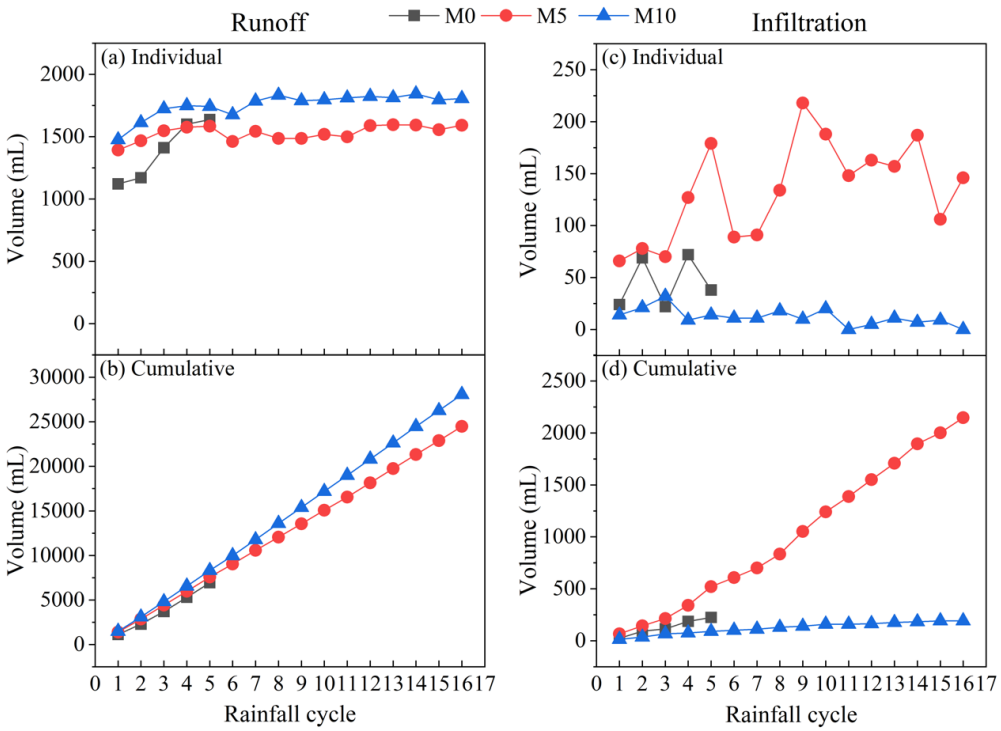

497

498 Fig. 2. Runoff (a-individual, b-cumulative) and infiltration (c-individual, d-cumulative)

499 volumes of the soils with and without MgO treatment.

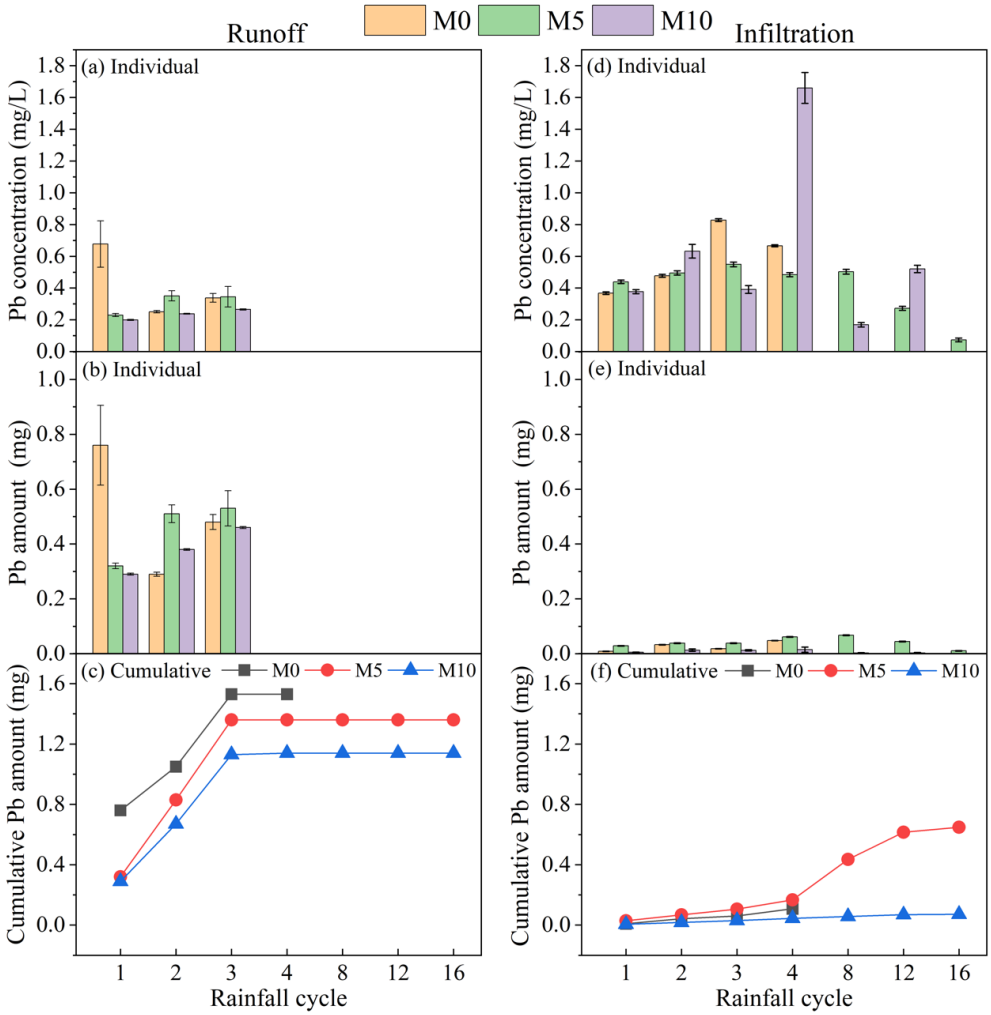

Fig. 3. Pb leaching in the runoff (a-individual concentration, b-individual amount, c-cumulative amount) and infiltration (c-individual concentration, d-individual amount, f-cumulative amount).

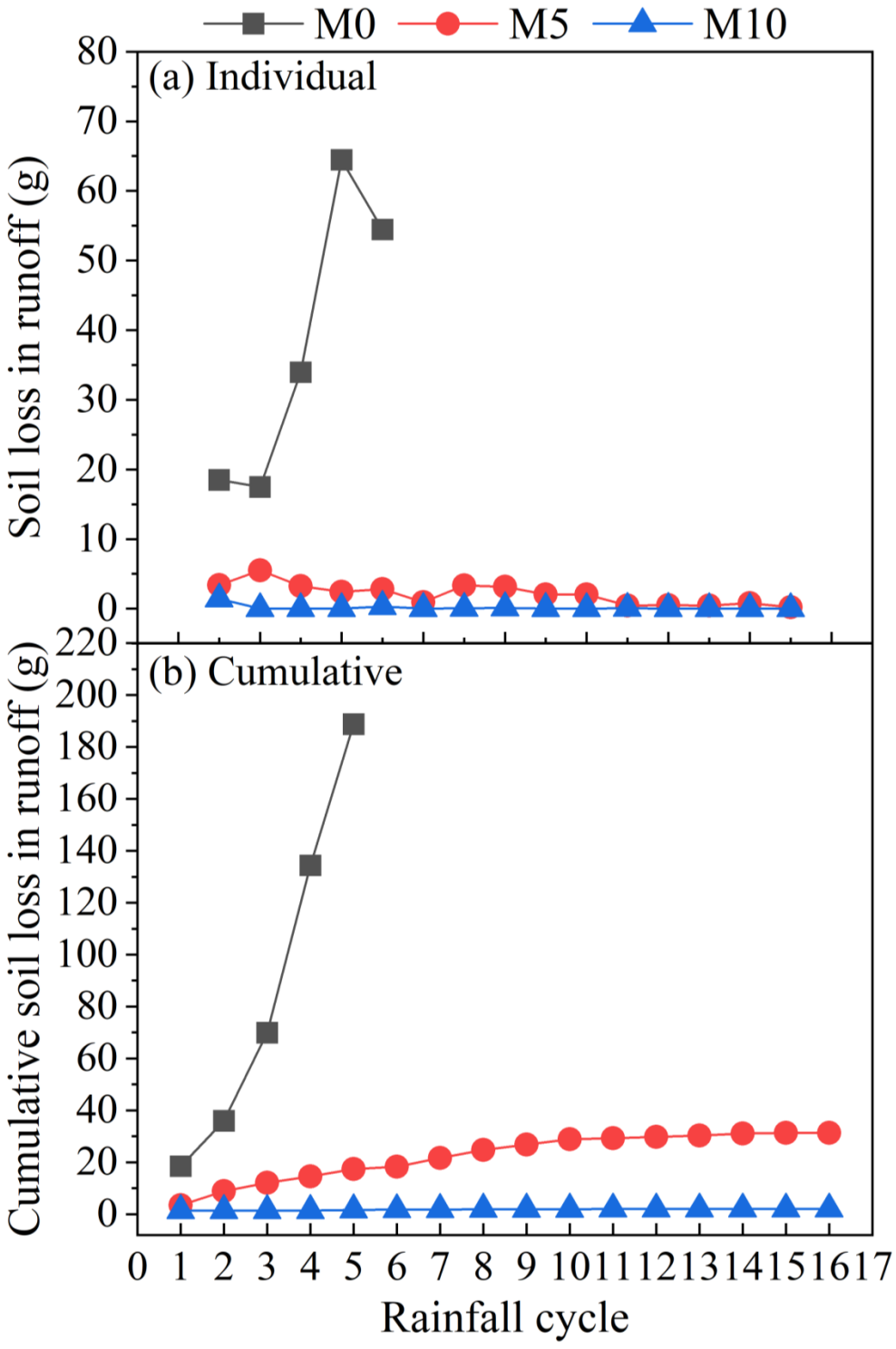

504

505 Fig. 4. Erosion induced loss of Pb-contaminated soil (a-individual rainfall, b-cumulative).

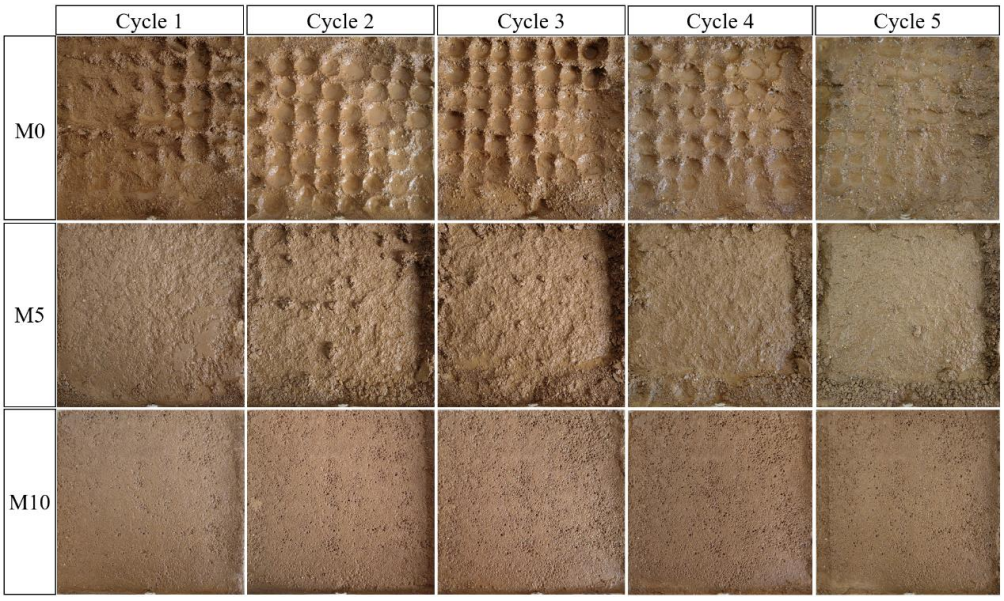

Fig. 5. Effect of MgO on surface morphology of Pb-contaminated soil during rainfall cycles.

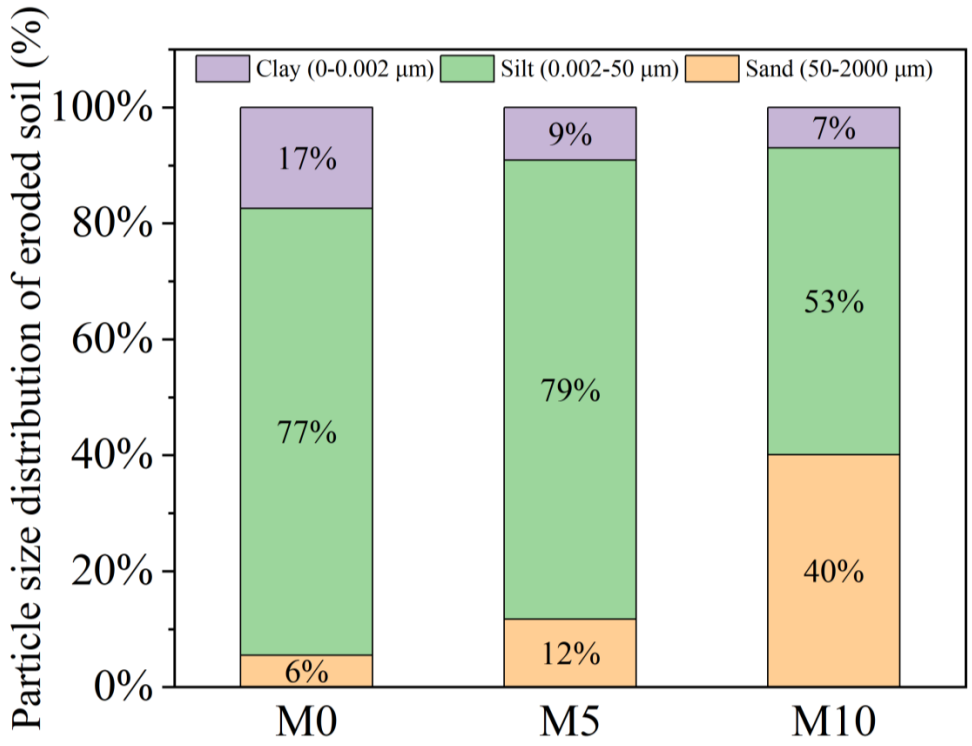

508

509

510 Fig. 6. Particle size distribution of the eroded Pb-contaminated soil in runoff.

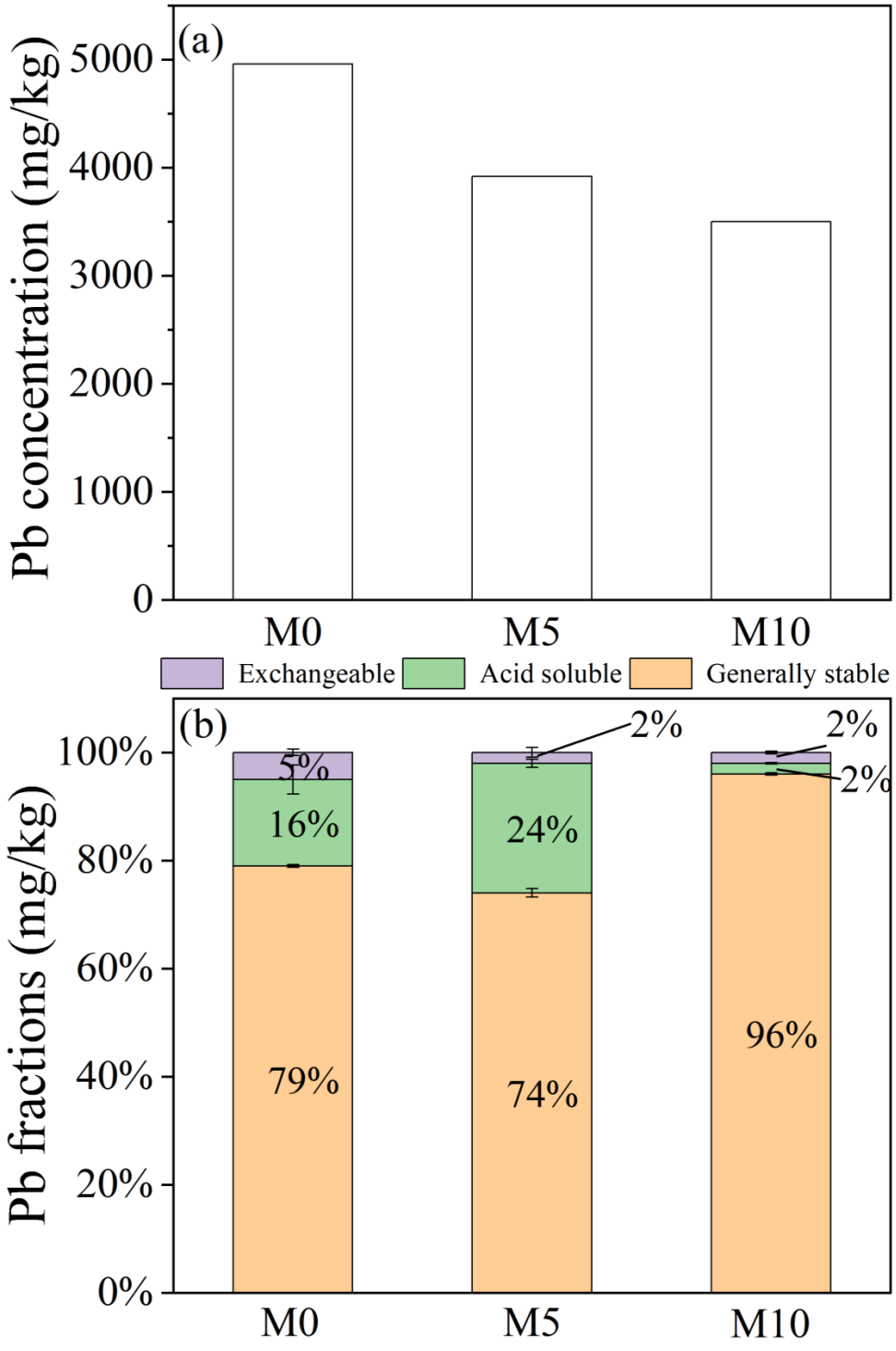

Fig. 7. Pb concentration (a) and fraction (b) of eroded soil in runoff.

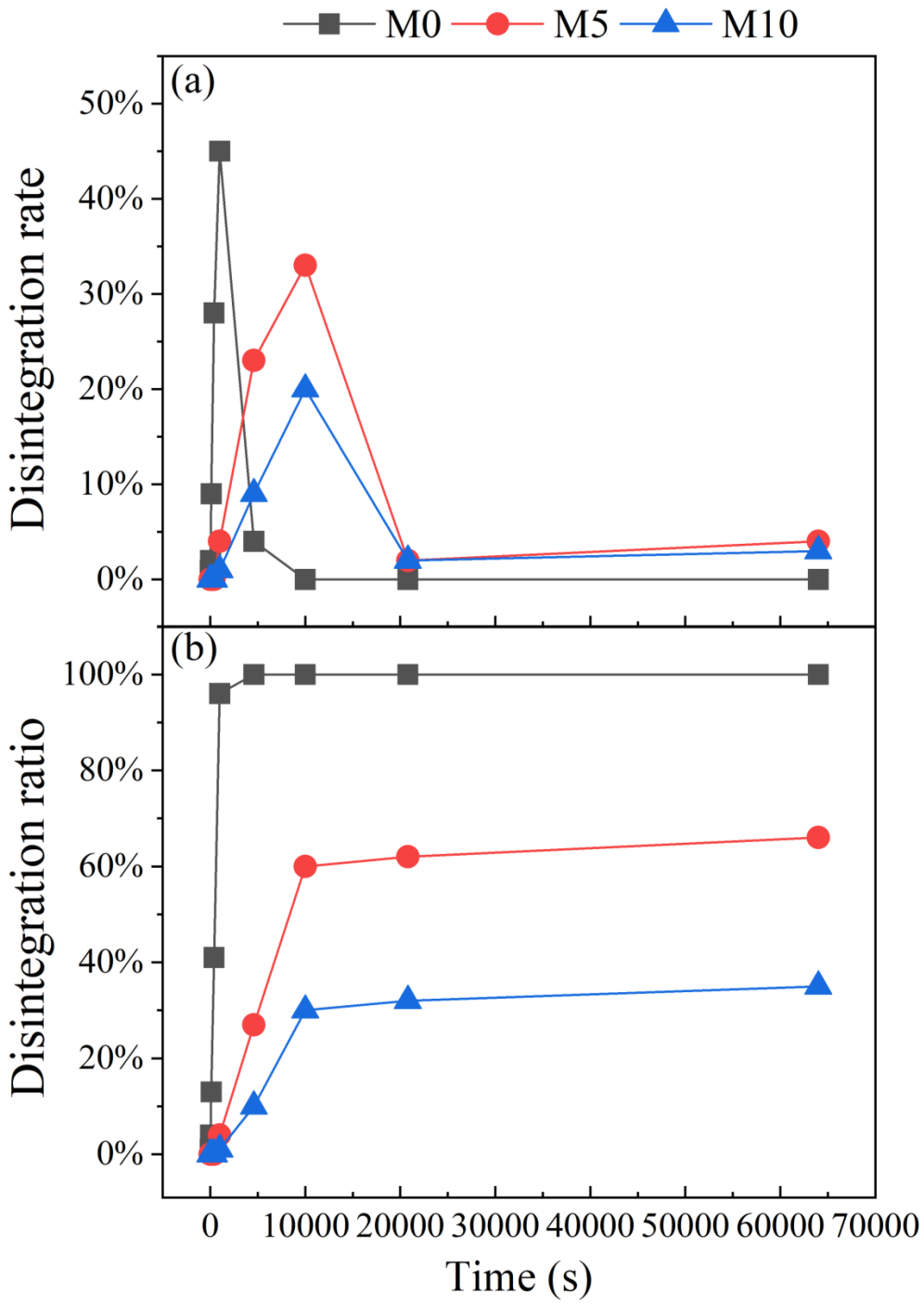

513

514 Fig. 8. Disintegration rate (a) and ration (b) of Pb contaminated soil.